Piezo2 channel regulates RhoA and actin cytoskeleton to promote cell mechanobiological responses

Carlos Pardo-Pastor[a], Fanny Rubio-Moscardo[a], Marina Vogel-González[a], Selma A. Serra[a], Alexandros Afthinos[b,c], Sanela Mrkonjic[d], Olivier Destaing[d], Juan F. Abenza[e], José M. Fernández-Fernández[a], Xavier Trepat[e,f], Corinne Albiges-Rizo[d], Konstantinos Konstantopoulos[b,c], and Miguel A. Valverde[a,1]

[a]Laboratory of Molecular Physiology, Department of Experimental and Health Sciences, Universitat Pompeu Fabra, 08003 Barcelona, Spain; [b]Department of Chemical and Biomolecular Engineering, Johns Hopkins University, Baltimore, MD 21218; [c]Institute for NanoBioTechnology, Johns Hopkins University, Baltimore, MD 21218; [d]Institute for Advanced Sciences, CRNS UMR 5309, INSERM U1209, Institut Albert Bonniot, University Grenoble Alpes, Site Santé, 5588 Grenoble, France; [e]Institute for Bioengineering of Catalonia, Facultat de Medicina, Universitat de Barcelona and Ciber Enfermedades Respiratorias, 08028 Barcelona, Spain; and [f]Institució Catalana de Recerca i Estudis Avançats, 08010 Barcelona, Spain

Edited by Ramon Latorre, Universidad de Valparaíso, Valparaíso, Chile, and approved January 12, 2018 (received for review October 17, 2017)

Actin polymerization and assembly into stress fibers (SFs) is central to many cellular processes. However, how SFs form in response to the mechanical interaction of cells with their environment is not fully understood. Here we have identified Piezo2 mechanosensitive cationic channel as a transducer of environmental physical cues into mechanobiological responses. Piezo2 is needed by brain metastatic cells from breast cancer (MDA-MB-231-BrM2) to probe their physical environment as they anchor and pull on their surroundings or when confronted with confined migration through narrow pores. Piezo2-mediated Ca^{2+} influx activates RhoA to control the formation and orientation of SFs and focal adhesions (FAs). A possible mechanism for the Piezo2-mediated activation of RhoA involves the recruitment of the Fyn kinase to the cell leading edge as well as calpain activation. Knockdown of Piezo2 in BrM2 cells alters SFs, FAs, and nuclear translocation of YAP; a phenotype rescued by overexpression of dominant-positive RhoA or its downstream effector, mDia1. Consequently, hallmarks of cancer invasion and metastasis related to RhoA, actin cytoskeleton, and/or force transmission, such as migration, extracellular matrix degradation, and Serpin B2 secretion, were reduced in cells lacking Piezo2.

mechanotransduction | calcium signaling | RhoA | actin stress fibers | cancer

Cancer cells invading and metastasizing away from the primary tumor encounter diverse physical constraints. To overcome these hurdles, they usually orchestrate mechanical and chemical signals to control cytoskeletal dynamics (1), cell volume (2, 3), degradation of extracellular matrix (ECM) (4), extravasation (5), confined migration (6, 7), and survival in distant organs (8). Besides, MDA-MB-231-BrM2 (BrM2 for short) breast cancer cells that specifically metastasize in the brain use Serpins to protect themselves from death signals generated by the reactive brain stroma (9). All these cellular functions involve mechanical interaction with the environment and, therefore, are amenable to be modulated by mechanosensitive Piezo channels (10) that transduce mechanical stimuli into intracellular signals, typically increasing intracellular Ca^{2+} concentration. Indeed, functional expression of Piezo channels has been described in malignant breast cancer cell lines (11), although their relevance to cancer has not been identified yet. Piezo1 modulates integrin activity (12), senses changes in the rigidity of the environment (13) and cell overcrowding (14), and optimizes confined migration (7), whereas Piezo2 channel participates in sensing gentle touch (15) and proprioception (16, 17). We herein set to decipher the potential roles of Piezo channels in the acquisition of the mechanobiological properties of BrM2 cells.

Results and Discussion

Increased Expression of Piezo2 Channel in BrM2 Cells. We first analyzed the expression of Piezo1 and Piezo2 channels in MDA-MB-231 cells. Compared with the parental MDA-MB-231 cells, Piezo2 was up-regulated in BrM2 cells with little change in Piezo1 mRNAs (Fig. 1*A*). As previously reported (9), BrM2 cells showed increased expression of Serpins (Fig. S1*A*). We used small hairpin RNA to suppress Piezo2 expression (shPiezo2). Quantitative RT-PCR analysis showed that Piezo2 expression was reduced (Fig. 1*B*) without affecting the expression of Piezo1 or other mechano/osmosensitive ion channels (TRPC1, TRPM7, TRPV4, and LRRC8A) (Fig. S1*B*) involved in different aspects of cell migration (3, 18). Patch-clamp recordings of whole-cell cation currents showed that Piezo2 knockdown (KD) reduced currents elicited by mechanical stimulation (Fig. 1 *C* and *D*) and decreased their inactivation (Fig. 1*E*), consistent with the faster inactivation kinetics of Piezo2 channel (10).

Piezo2 Is Needed by BrM2 Cells to Probe Their Physical Environment. One typical mechanobiological response of cells growing on solid surfaces is their ability to anchor and pull on the substrate. Therefore, we studied the traction forces generated by BrM2 cells on polyacrylamide gels of different rigidities. Traction forces are generated by myosin II and require both the integrity of the actin cytoskeleton and focal adhesions (FAs) through which cells transmit the force to their substratum (19, 20). BrM2-shControl cells exerted higher traction forces on stiffer substrates, whereas BrM2-shPiezo2 cells generated low traction forces that were insensitive to substrate stiffness (Fig. 1 *F* and *G*). The effect of knocking down Piezo2 on traction forces was

Significance

The actin cytoskeleton is central to many cellular processes involving changes in cell shape, migration, and adhesiveness. Therefore, there is a great interest in the identification of the signaling pathways leading to the regulation of actin polymerization and assembly into stress fibers (SFs). However, to date it is not well understood how the mechanical interactions between cells and their environment activate the assembly of SFs. Here, we demonstrate that the mechanosensitive Piezo2 channel is required to sense physical cues from the environment to generate a calcium signal that maintains RhoA active and the formation and orientation of SFs and focal adhesions. Besides, this Piezo2-initiated signaling pathway has implications for different hallmarks of cancer invasion and metastasis.

Author contributions: C.P.-P., C.A.-R., K.K., and M.A.V. designed research; C.P.-P., F.R.-M., M.V.-G., S.A.S., A.A., S.M., O.D., and J.F.A. performed research; C.P.-P., S.A.S., J.M.F.-F., X.T., C.A.-R., K.K., and M.A.V. analyzed data; and M.A.V. wrote the paper.

The authors declare no conflict of interest.

This article is a PNAS Direct Submission.

[1]To whom correspondence should be addressed. Email: miguel.valverde@upf.edu.

This article contains supporting information online at www.pnas.org/lookup/suppl/doi:10.1073/pnas.1718177115/-/DCSupplemental.

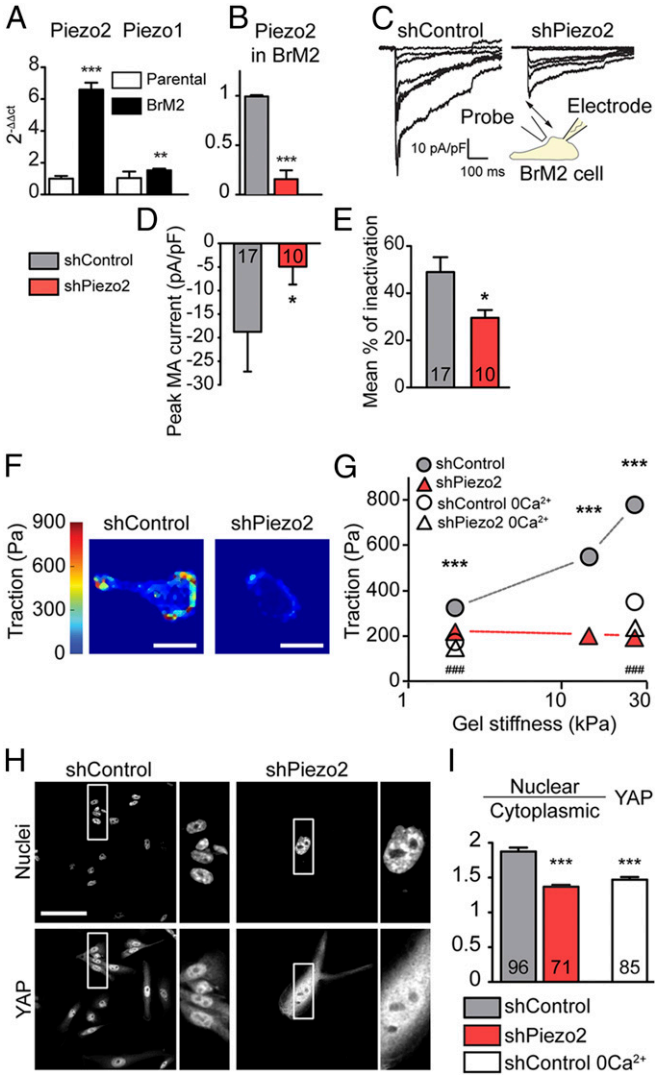

Fig. 1. Piezo2 is required for force transmission and mechanotransduction in MDA-MB-231-BrM2 cells. (*A*) Quantitative real-time PCR (qPCR) of Piezo1 and -2 expression in parental and MDA-MB-231-BrM2 cells, $n = 3$. (*B*) qPCR of Piezo2 in shControl and shPiezo2 BrM2 cells, $n = 3$. (*C*) Representative whole-cell traces of mechanically activated (MA) inward cationic currents recorded at a holding potential of −80 mV from BrM2-shControl and BrM2-shPiezo2 cells following stimulation with a series of mechanical steps of 0.5 μm (*Inset* illustration). (*D*) Peak MA current density and (*E*) percentage of MA current inactivation in BrM2-shControl and BrM2-shPiezo2 cells. (*F*) Color map images of traction forces exerted by cells on 15-kPa hydrogels. (Scale bar, 20 μm.) (*G*) Mean traction forces obtained at 2 (shControl $n = 103$; shPiezo2 $n = 110$), 15 (shControl $n = 51$; shPiezo2 $n = 38$), and 30 kPa (shControl $n = 72$; shPiezo2 $n = 56$), and at 2 (shControl $n = 51$; shPiezo2 $n = 41$) and 30 kPa (shControl $n = 27$; shPiezo2 $n = 25$) in the absence of extracellular Ca^{2+}. $^{***}P < 0.001$ shPiezo2 vs. shControl for each stiffness. $^{\#\#\#}P < 0.001$ shControl vs. shControl $0Ca^{2+}$. (*H*) Nuclear and YAP stainings of cells seeded on glass. White rectangles define the zoomed region. (Scale bar, 50 μm.) (*I*) Mean YAP nuclear/cytoplasmic signal ratio. The number of cells analyzed for each condition is indicated in each bar. $^{*}P < 0.05$, $^{**}P < 0.01$, and $^{***}P < 0.001$.

phenocopied in BrM2-shControl cells cultured in the absence of extracellular Ca^{2+} (Fig. 1*G*). In agreement with lower traction forces, BrM2-shPiezo2 cells presented faster retrograde actin flow at the leading edge (Fig. S2 *A* and *B*) and larger surface areas (Fig. S2*C*).

To analyze the impact of Piezo2-KD on cellular adaptation to the physical microenvironment, we studied the mechanosensitive transcriptional regulator YAP involved in breast cancer biology (21) and known to sense cytoskeletal tension by responding with its nuclear translocation (22). In accordance with the traction forces data, BrM2-shPiezo2 cells presented less nuclear accumulation of YAP than BrM2-shControl cells (Fig. 1 *H* and *I*). Similarly, removal of extracellular Ca^{2+} reduced nuclear accumulation of YAP in BrM2-shControl cells (Fig. 1*I*). No significant differences in total or phosphorylated YAP levels were detected between BrM2-shControl and BrM2-shPiezo2 cells (Fig. S3 *A* and *B*), which agrees with previous reports showing that YAP phosphorylation is not essential for its nuclear translocation under mechanical stimulation (23). Consistent with lower nuclear signal of YAP, BrM2-shPiezo2 cells proliferate slower than control cells (Fig. S3*C*) and the expression of a YAP/TAZ target gene, the connective tissue growth factor (*CTGF*) gene, that increased in BrM2 cells was returned back to parental MDA-231-MB cell level following Piezo2-KD (Fig. S3*D*). Together, our data suggest that Piezo2 plays a key role in the ability of BrM2 cells to sense and transduce mechanical cues and open the question of how Piezo2 participates in those processes.

Piezo2 Controls Formation of Actin-Based Stress Fibers and Orientation of Focal Adhesions. The three main players in mechanical sensing/transduction, actin-based stress fibers (SFs), FAs, and myosin, are also modulated by the intracellular Ca^{2+} concentration (24, 25). However, the underlying molecular mechanism of SF generation after environment–cell contact and the Ca^{2+} dependency of such a process are largely unknown. Well-defined SFs were observed in BrM2-shControl cells but were absent in BrM2-shPiezo2 cells (Fig. 2 *A* and *B*). Similarly, BrM2-shControl cells cultured in Ca^{2+}-free medium lacked SFs (Fig. 2 *A* and *B*), consistent with a role of Piezo2 in the generation of the Ca^{2+} signal required for SF formation. The actin polymerizing drug, jasplakinolide, which bypasses the physiologically regulated actin polymerization, rescued the effect of Piezo2-KD on the actin cytoskeleton (Fig. 2 *A* and *B*).

SFs anchor to the membrane at FAs, providing a mechanical path to sense and generate traction forces in adherent cells. Therefore, formation and maturation of FAs and SFs are intimately linked and related, at least in part, to the generation of mechanical tension (26). We detected FAs using an antibody against the adaptor protein Paxillin. FAs were elongated, polarized, and oriented along the major axis of BrM2-shControl cells, whereas FAs were more puncta type and randomly distributed across the entire area of BrM2-shPiezo2 cells (Fig. 2*C*). Removal of extracellular Ca^{2+} also induced the presence of smaller and more disperse FAs in control cells (Fig. 2*C*), whereas jasplakinolide promoted the presence of elongated, polarized, and oriented FAs in BrM2-shPiezo2 cells (Fig. 2*C*). Quantification of the FA angle in respect to the major cell axis (Fig. 2*D*) illustrates that Piezo2-KD promoted FAs that appear more radially oriented (higher percentage of FAs showing angles close to 90° in BrM2-shPiezo2 cells than in control cells), a phenotype that was reverted with jasplakinolide. An independent shRNA targeting Piezo2 replicated the results obtained thus far (Fig. S4).

Further support to the relevance of Piezo2 channel in the regulation of actin dynamics and SF formation was obtained by immunolocalizing Piezo2 and Paxillin. Piezo2 signal was clearly identified at the cell boundary. Colocalization of Piezo2 with Paxillin signals was present at the FA of the leading edge in BrM2-shControl cells while in BrM2-shPiezo2 cells the Piezo2 signal was almost undetectable and, therefore, no colocalization was observed (Fig. 2*E*). This observation is in line with a previous report showing the contribution of stretch-activated ion channels to the generation of traction forces at the leading edge of fibroblasts (27). The impact of Piezo2 knockdown on other elements of the machinery involved in sensing and transducing mechanical cues was also tested by means of Western blotting of activated proteins.

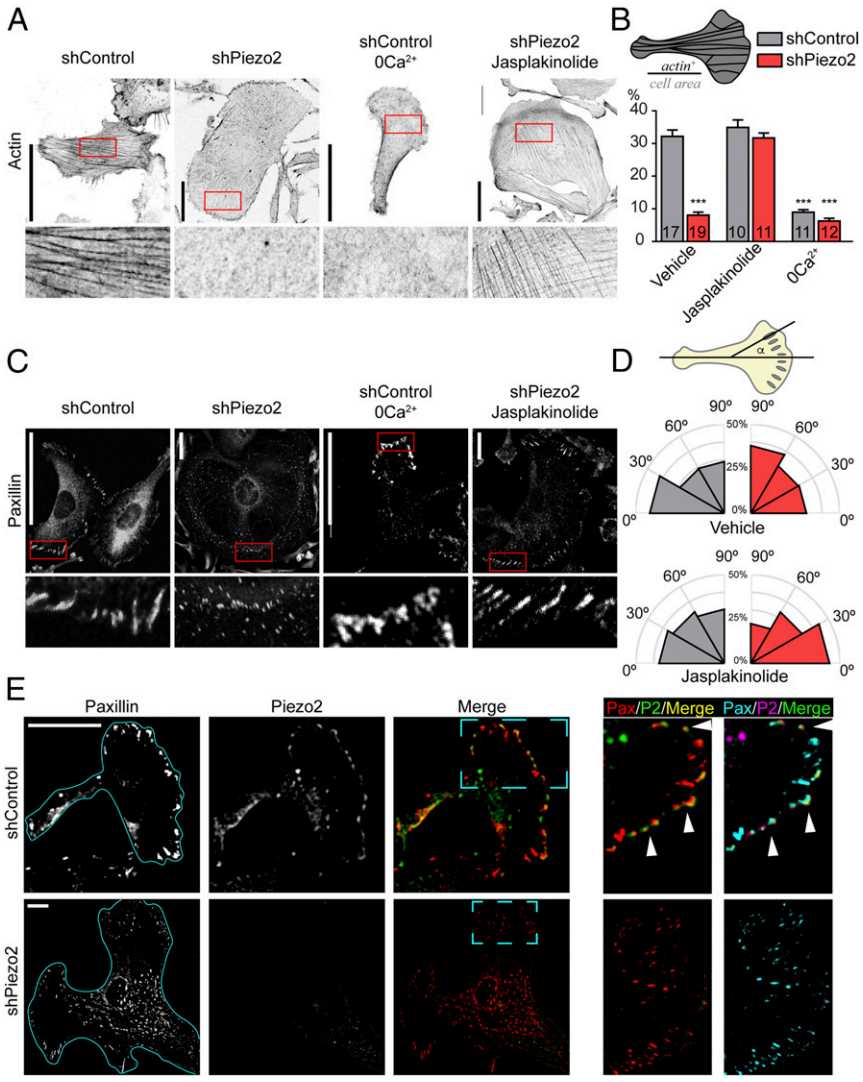

Fig. 2. Ca^{2+} entry via Piezo2 regulates the actin cytoskeleton and adhesions. (*A*) Representative maximal intensity projections of whole-cell Z scans of phalloidin-stained actin in cells treated as indicated. (*B*) Mean percentage of total cell area occupied by actin. (*C*) Paxillin staining of the basal planes of cells. (*D*) Rose plot of the angles of adhesions respective to the cell major axis. (*Top*) DMSO, (*Bottom*) 500 nM jasplakinolide. (Scale bar, 50 μm.) Red rectangles define the zoomed region. ***$P < 0.001$. (*E*) Immunofluorescence confocal microscopy images of Piezo2 and Paxillin. Note the strong reinforcement of Piezo2 signal at the cell boundary of BrM2-shControl cells and the almost total absence of Piezo2 signal in BrM2-shPiezo2 cells. The merge panel displays the colocalization between Piezo2 and Paxillin. Magnified views of the respective boxes drawn at the cell leading edges are shown on the *Right* with two combinations of colors to facilitate viewing by color-blinded people. Arrowheads marked colocalization of Piezo2 and Paxillin at FA of the leading edge in shPiezo2 cells.

BrM2-shPiezo2 cells showed no significant changes in phosphorylated myosin light chain (pMLC) (Fig. S5*A*), consistent with the unaltered myosin-dependent retrograde actin flow (28) recorded in BrM2-shPiezo2. Similarly, no changes on phosphorylated focal adhesion kinase (pFAK) were detected in BrM2-shPiezo2 compared with BrM2-shControl cells (Fig. S5*B*).

Piezo2-KD Reduces RhoA Activity in BrM2 Cells. The question that came up next was how Piezo2 activity drives actin polymerization and SF formation. SFs are assembled in response to a signaling cascade involving RhoA (29). RhoA activity increases with force application (30–32), although little is known about the mechanical activation of RhoA in the absence of externally applied forces. To evaluate whether Piezo2 is an upstream regulator of RhoA, we measured RhoA activity in control and Piezo2-KD cells using a fluorescence resonance energy transfer (FRET)-based RhoA sensor (33). FRET images in Fig. 3*A* revealed a significant decrease in RhoA activity in BrM2-shPiezo2 cells compared with BrM2-shControl cells (Fig. 3 *A* and *B*) without differences in RhoA protein levels (Fig. 3*C*). RhoA activity increases in response to activation of receptors/channels that promote Ca^{2+} influx (34–37). Accordingly, removal of extracellular Ca^{2+} reduced RhoA activity in BrM2-shControl cells to the values recorded in BrM2-shPiezo2 cells (Fig. 3*B*), suggesting that Piezo2 regulates RhoA activity through the generation of an intracellular Ca^{2+} signal. The link between RhoA and Piezo2 in the regulation of actin cytoskeleton was further confirmed by showing that transfection of the RhoA-T19N dominant-negative plasmid (38) into BrM2-shControl cells mimicked the shPiezo2 phenotype, whereas expression of the RhoA-Q63L dominant positive plasmid (38) restored the presence of SFs (Fig. 3 *D* and *E*) and the nuclear accumulation of YAP in BrM2-shPiezo2 cells (Fig. 3 *F* and *G*). The formin mDia1, activated downstream of RhoA, is the ultimate effector that drives actin polymerization (39, 40). Expression of a dominant-positive mDia1 (CAmDia1) in BrM2-shPiezo2 cells also rescued the control SF phenotype (Fig. 3 *D* and *E*) and nuclear accumulation of YAP (Fig. 3 *F* and *G*).

In an attempt to elucidate the molecular mechanisms that link Piezo2 with RhoA activity, we focused on the Src family tyrosine kinase, Fyn. Fyn participates in the formation of SFs and in response to mechanical stimulation activates the guanine nucleotide exchange factor (GEF) LARG, which in turn activates RhoA (32, 41–43). Besides, Fyn can be activated by increases in intracellular Ca^{2+} concentration (44) and has to be recruited to the adhesion complexes at the cell leading edge to play a role in ECM rigidity and mechanical sensing (41). BrM2-shControl cells showed a clear colocalization of Fyn and the FA marker, pFAK, mainly on the leading edge (Fig. 4*A*), with a Manders' correlation coefficient of ∼0.75 (Fig. 4*B*). No such correlation was found in BrM2-shPiezo2 cells (Fig. 4 *A* and *B*), suggesting higher

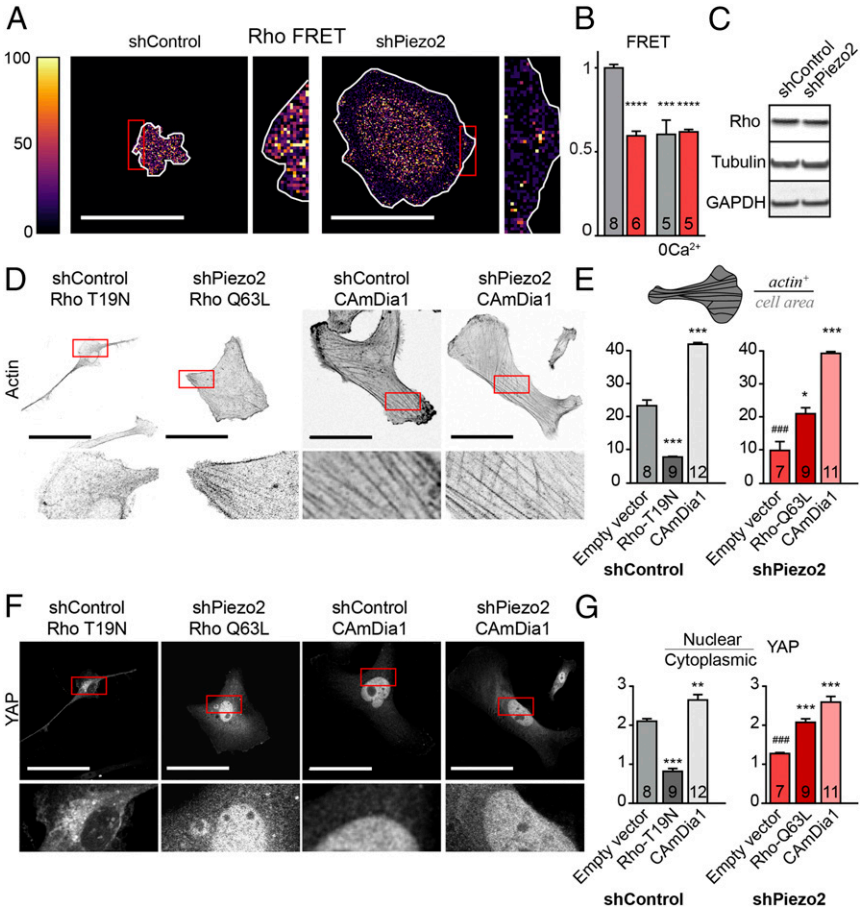

Fig. 3. The Piezo2-RhoA-mDia1 axis controls actin polymerization and mechanotransduction. (*A*) FRET/CFP emission ratio measurements of Raichu-RhoA sensor transfected BrM2 cells. (Scale bar, 25 μm.) (*B*) Normalized mean FRET/CFP ratio of the whole-cell areas measured in the presence and in the absence of extracellular Ca^{2+}. (*C*) Western blot of total lysates obtained from shControl and shPiezo2 BrM2 cells and probed with anti-RhoA, anti-tubulin, and anti-GAPDH antibodies. (*D* and *F*) Representative maximal intensity projections of whole-cell Z scans of phalloidin-marked actin (*D*) or YAP (*F*) in cells transfected with the indicated plasmids. (*E*) Mean percentage of total cell area occupied by actin. (*G*) Mean YAP nuclear/cytoplasm ratio. Red rectangles define the zoomed region. (Scale bar, 50 μm.) $^{*}P < 0.05$, $^{**}P < 0.01$, $^{***}P < 0.001$, $^{****}P < 0.0001$ relative to shControl (*B*), empty vector shControl (*E* and *G*, *Left*) or empty vector shPiezo2 (*E* and *G*, *Right*). $^{\#\#\#}P < 0.001$ relative to empty vector shControl cells.

Fyn activity in BrM2-shControl than in BrM2-shPiezo2 cells. No changes in total Fyn were detected between BrM2-shControl and BrM2-shPiezo2 cells (Fig. 4*C*).

Another signaling molecule that may link Piezo2-induced Ca^{2+} signals to the activation of RhoA is calpain. Calpains are Ca^{2+}-dependent intracellular proteases that regulate FA dynamics (45)

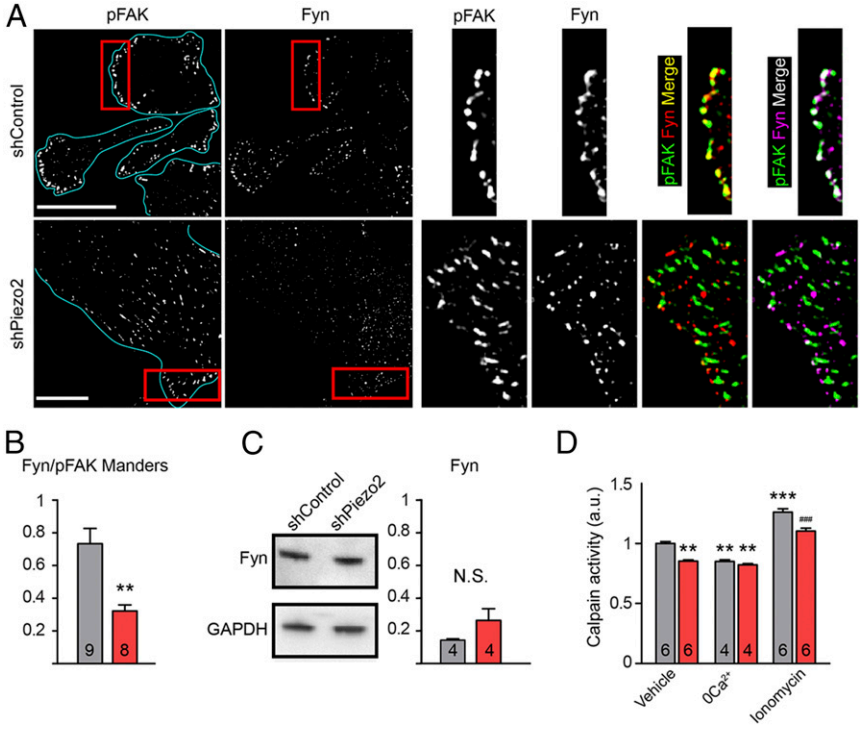

Fig. 4. Fyn localization and calpain activity is altered in BrM2-shPiezo2 cells. (*A*) Immunofluorescence confocal microscopy images of phosphorylated FAK (pFAK, marker of FA) and Fyn. Contour of cells is marked by a blue line. Magnified views of the respective boxes drawn at the cell leading edges are shown on the *Right* with two combinations of colors to facilitate viewing by color-blinded people. Note the colocalization of pFAK and Fyn signals at the leading edge of BrM2-shControl cells that is absent in BrM2-shPiezo2 cells. (*B*) Quantification of the Fyn/pFAK colocalization using Manders' coefficient. (*C*) Representative images of Western blots (*Left*) and quantification of Fyn normalized to GAPDH levels (*Right*). (*D*) Calpain activity (measured using a permeant nonfluorescent substrate of calpain that becomes fluorescent upon calpain-mediated cleavage) is reduced in vehicle-treated shPiezo2 cells compared with shControl cells. Removal of extracellular calcium ($0Ca^{2+}$) reduced calpain activity, whereas the presence of the calcium ionophore ionomycin (1 μM) increased it. $^{**}P < 0.01$, $^{***}P < 0.001$ relative to shControl vehicle. $^{\#\#\#}P < 0.001$ relative to vehicle shPiezo2 condition. N.S., not significant.

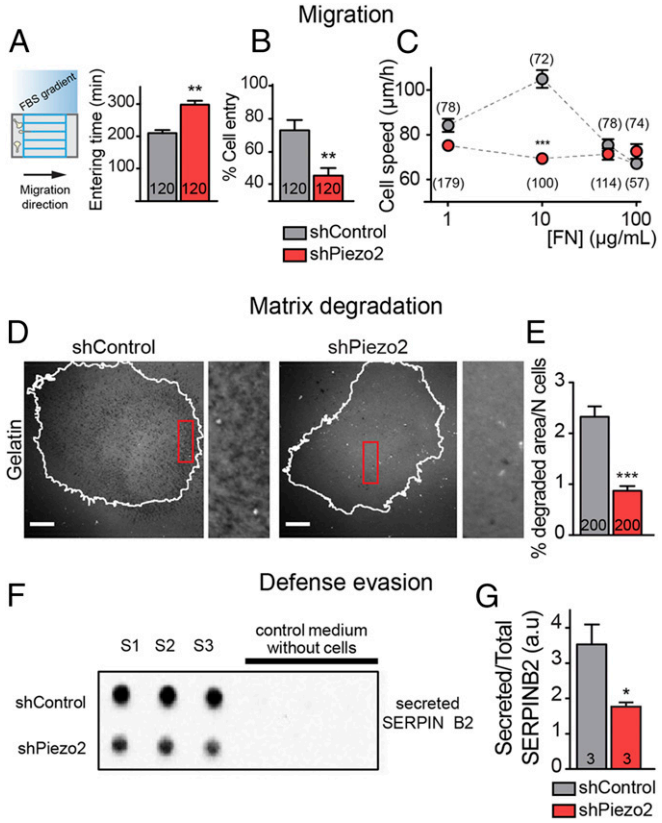

Fig. 5. Piezo2 knockdown impairs brain metastasis-favoring functions. (*A*) Mean time needed to enter 3 μm-wide channels and (*B*) mean percentage of cells achieving it. (*C*) Mean speeds of cells migrating at different fibronectin-coating concentrations. (*D*) Images of fluorescent gelatin substrates. White lines define the cell contour. Red rectangles define the zoomed region. (Scale bar, 10 μm.) (*E*) Mean percentage of degraded area relative to the number of cells. (*F*) Dot blot of supernatants collected from three independent wells containing shControl and shPiezo2 BrM2 cells probed with anti-SERPIN2 B2 antibody. (*G*) SERPIN B2 secretion normalized to total SERPIN B2. $*P < 0.05$, $**P < 0.01$, $***P < 0.001$.

as well as RhoA activity (46) and SF formation (47). Calpain activity was reduced in BrM2-shPiezo2 cells compared with BrM2-shControl cells (Fig. 4*D*). To confirm that the difference in calpain activity was due to reduced Ca^{2+} influx in BrM2-shPiezo2 cells, we measured calpain activity in the absence of extracellular Ca^{2+} or in the presence of the Ca^{2+} ionophore ionomycin. Removal of extracellular Ca^{2+} reduced calpain activity only in BrM2-shControl cells, whereas addition of ionomycin increased calpain activity in both control and shPiezo2 cells (Fig. 4*D*). Together, we postulate that a Piezo2-generated Ca^{2+} signal is an upstream regulator of the RhoA-mDia pathway necessary for the homeostatic regulation of actin cytoskeleton and force sensing/transduction in BrM2 cells. It will be interesting in the future to investigate the relative contribution of Fyn and calpain and whether other Ca^{2+} signaling pathways also participate in the Piezo2-mediated activation of RhoA.

Piezo2 Modulates Different Mechanobiological Responses of BrM2 Cells. Piezo2 is expressed in both normal and breast cancer tissue (ref. 48; www.proteinatlas.org), and is overexpressed (Fig. 1) in the MDA-MB-231-BrM2 cells from breast cancer that specifically metastasize in the brain (9). Besides, analysis of existing breast cancer databases (49) suggested that low expression of Piezo2 implied a statistically significant longer survival rate of patients with breast cancers (Fig. S6) that, like the MDA-231-MB-BrM2 cells, were negative for the estrogen, progesterone, and human epidermal growth factor 2 receptors (triple negative cancers). The mechanotransducing elements that regulate cytoskeletal dynamics and cell–matrix interactions confer plasticity and rapid adaptation to invading cells (50, 51). Moreover, actin remodeling influences cancer drug resistance (52). Therefore, we tested the impact of Piezo2-KD on different mechanobiological responses that may confer BrM2 cells with an advantage to invade and metastasize in the brain, i.e., their ability to: (*i*) migrate in confined environments, (*ii*) remodel ECM, and (*iii*) develop defense evasion strategies.

When challenged to migrate through 3-μm narrow microfabricated channels (Fig. S7 *A* and *B*) to mimic the pores encountered by metastatic breast cancer cells (6), BrM2-shPiezo2 cells required longer times to enter channels and fewer cells entered the channels compared with BrM2-shControl cells (Fig. 5 *A* and *B*), although speed and persistence within the channels were not affected (Fig. S7*C*). Cells exhibit a biphasic dependence of migration velocity with increasing adhesion strength on 2D planar surfaces. This phenomenon, known as haptotaxis, implies that maximal velocity is obtained at intermediate adhesion strength (i.e., intermediate fibronectin concentration in the extracellular matrix) and depends on the dynamic organization of actin, FAs, and myosin (53). Knockdown of Piezo2 abrogated haptotaxis in BrM2 cells (Fig. 5*C*).

Cancer cells often use specialized adhesive structures named invadosomes to make contact with the ECM and degrade it, thereby promoting invasion and metastasis (4, 5). These actin-based cellular protrusions also required active Rho for proper functioning (54). To investigate the role of Piezo2 in invadosome function, we tested the ability of BrM2 cells to degrade a fluorescent gelatin substrate. Degradation of ECM was detected by the appearance of nonfluorescent gelatin patches underneath the cells (Fig. 5*D*) that colocalize with the actin core of invadosomes (Fig. S8). BrM2-shPiezo2 cells showed reduced gelatin degradation (Fig. 5*E*) compared with BrM2-shControl cells.

The expression of Serpins is increased in BrM2 cells, conferring them an advantage to survive and metastasize in the brain (9). Serpins act extracellularly by inhibiting the plasminogen activator, although little is known about the mechanism of Serpin secretion. Considering that both Ca^{2+}- and Rho-mediated signaling is typically associated with regulated secretion (55, 56) we wondered whether Piezo2 channel participates in the release of Serpin B2. Compared with control cells, BrM2-shPiezo2 cells presented reduced Serpin B2 secretion (Fig. 5 *F* and *G* and Fig. S9).

In conclusion, Piezo2 is needed by brain metastatic cells from breast cancer, MDA-MB-231-BrM2 cells, to probe their physical environment. The Piezo2-generated Ca^{2+} signal activates downstream the RhoA-mDia pathway necessary for the regulation of actin cytoskeleton. The generality and relevance of this mechanism in other cell/tissue contexts need to be tested but it is tempting to speculate that it may be relevant during development, when mechanical forces are involved in patterning and organogenesis. In this regard, it is worth mentioning that *PIEZO2* mutations have been linked to developmental malformations (57, 58). Finally, the Piezo2-mediated force sensing/transduction confers BrM2 cells advantages in relation to their ability to proliferate, invade, migrate in confined environments, and survive in the brain, offering an interesting target for therapeutic intervention.

Materials and Methods

All experiments were performed on parental, MDA-MB-231, and MDA-MB-231-BrM2 breast cancer cells that specifically metastasize in the brain (9). Further details on cell-culture conditions, shRNA knockdown of Piezo2, gel fabrication, confocal immunofluorescence localization, cell migration, RhoA

PHYSIOLOGY

activity, calpain activity, electrophysiological and traction force measurements, and data analysis are presented in *SI Materials and Methods*.

ACKNOWLEDGMENTS. The research is supported by the Spanish Ministry of Economy and Competitiveness (Grants SAF2015-69762-R to M.A.V. and J.M.F.-F., and MDM-2014-0370 through the "María de Maeztu" Programme for Units of Excellence in R&D to "Departament de Ciències Experimentals i de la Salut"); Fondo Europeo de Desarrollo Regional; European Project 658902-OSS and Fondation pour la Recherche Médicale en France DEQ20170336702 (to C.A.-R.); and National Institutes of Health National Cancer Institute Grant R01 CA183804 and National Institute of General Medical Sciences Grant R01 GM114675 (to K.K.).

1. Ridley AJ, et al. (2003) Cell migration: Integrating signals from front to back. *Science* 302:1704–1709.
2. Watkins S, Sontheimer H (2011) Hydrodynamic cellular volume changes enable glioma cell invasion. *J Neurosci* 31:17250–17259.
3. Schwab A, Fabian A, Hanley PJ, Stock C (2012) Role of ion channels and transporters in cell migration. *Physiol Rev* 92:1865–1913.
4. Mrkonjic S, Destaing O, Albiges-Rizo C (2017) Mechanotransduction pulls the strings of matrix degradation at invadosome. *Matrix Biol* 57–58:190–203.
5. Leong HS, et al. (2014) Invadopodia are required for cancer cell extravasation and are a therapeutic target for metastasis. *Cell Rep* 8:1558–1570.
6. Stroka KM, et al. (2014) Water permeation drives tumor cell migration in confined microenvironments. *Cell* 157:611–623.
7. Hung WC, et al. (2016) Confinement sensing and signal optimization via Piezo1/PKA and myosin II pathways. *Cell Rep* 15:1430–1441.
8. Massagué J, Obenauf AC (2016) Metastatic colonization by circulating tumour cells. *Nature* 529:298–306.
9. Valiente M, et al. (2014) Serpins promote cancer cell survival and vascular co-option in brain metastasis. *Cell* 156:1002–1016.
10. Coste B, et al. (2010) Piezo1 and Piezo2 are essential components of distinct mechanically activated cation channels. *Science* 330:55–60.
11. Li C, et al. (2015) Piezo1 forms mechanosensitive ion channels in the human MCF-7 breast cancer cell line. *Sci Rep* 5:8364.
12. McHugh BJ, et al. (2010) Integrin activation by Fam38A uses a novel mechanism of R-Ras targeting to the endoplasmic reticulum. *J Cell Sci* 123:51–61.
13. Pathak MM, et al. (2014) Stretch-activated ion channel Piezo1 directs lineage choice in human neural stem cells. *Proc Natl Acad Sci USA* 111:16148–16153.
14. Eisenhoffer GT, et al. (2012) Crowding induces live cell extrusion to maintain homeostatic cell numbers in epithelia. *Nature* 484:546–549.
15. Woo S-H, et al. (2014) Piezo2 is required for Merkel-cell mechanotransduction. *Nature* 509:622–626.
16. Woo S-H, et al. (2015) Piezo2 is the principal mechanotransduction channel for proprioception. *Nat Neurosci* 18:1756–1762.
17. Florez-Paz D, Bali KK, Kuner R, Gomis A (2016) A critical role for Piezo2 channels in the mechanotransduction of mouse proprioceptive neurons. *Sci Rep* 6:25923.
18. Mrkonjić S, et al. (2015) TRPV4 participates in the establishment of trailing adhesions and directional persistence of migrating cells. *Pflugers Arch* 467:2107–2119.
19. Discher DE, Janmey P, Wang YL (2005) Tissue cells feel and respond to the stiffness of their substrate. *Science* 310:1139–1143.
20. Albiges-Rizo C, Destaing O, Fourcade B, Planus E, Block MR (2009) Actin machinery and mechanosensitivity in invadopodia, podosomes and focal adhesions. *J Cell Sci* 122:3037–3049.
21. Cordenonsi M, et al. (2011) The Hippo transducer TAZ confers cancer stem cell-related traits on breast cancer cells. *Cell* 147:759–772.
22. Dupont S, et al. (2011) Role of YAP/TAZ in mechanotransduction. *Nature* 474:179–183.
23. Elosegui-Artola A, et al. (2017) Force triggers YAP nuclear entry by regulating transport across nuclear pores. *Cell* 171:1397–1410.e14.
24. Burridge K, Guilluy C (2016) Focal adhesions, stress fibers and mechanical tension. *Exp Cell Res* 343:14–20.
25. Prevarskaya N, Skryma R, Shuba Y (2011) Calcium in tumour metastasis: New roles for known actors. *Nat Rev Cancer* 11:609–618.
26. Oakes PW, Beckham Y, Stricker J, Gardel ML (2012) Tension is required but not sufficient for focal adhesion maturation without a stress fiber template. *J Cell Biol* 196: 363–374.
27. Munevar S, Wang YL, Dembo M (2004) Regulation of mechanical interactions between fibroblasts and the substratum by stretch-activated Ca^{2+} entry. *J Cell Sci* 117: 85–92.
28. Vicente-Manzanares M, Ma X, Adelstein RS, Horwitz AR (2009) Non-muscle myosin II takes centre stage in cell adhesion and migration. *Nat Rev Mol Cell Biol* 10:778–790.
29. Ridley AJ, Hall A (1992) The small GTP-binding protein rho regulates the assembly of focal adhesions and actin stress fibers in response to growth factors. *Cell* 70:389–399.
30. Zhao X-H, et al. (2007) Force activates smooth muscle alpha-actin promoter activity through the Rho signaling pathway. *J Cell Sci* 120:1801–1809.
31. Goldyn AM, Rioja BA, Spatz JP, Ballestrem C, Kemkemer R (2009) Force-induced cell polarisation is linked to RhoA-driven microtubule-independent focal-adhesion sliding. *J Cell Sci* 122:3644–3651.
32. Guilluy C, et al. (2011) The Rho GEFs LARG and GEF-H1 regulate the mechanical response to force on integrins. *Nat Cell Biol* 13:722–727.
33. Aoki K, Matsuda M (2009) Visualization of small GTPase activity with fluorescence resonance energy transfer-based biosensors. *Nat Protoc* 4:1623–1631.
34. Sakurada S, et al. (2003) Ca^{2+}-dependent activation of Rho and Rho kinase in membrane depolarization-induced and receptor stimulation-induced vascular smooth muscle contraction. *Circ Res* 93:548–556.
35. Seminario-Vidal L, et al. (2011) Rho signaling regulates pannexin 1-mediated ATP release from airway epithelia. *J Biol Chem* 286:26277–26286.
36. Zhang L, et al. (2017) Calcium-sensing receptor stimulation in cultured glomerular podocytes induces TRPC6-dependent calcium entry and RhoA activation. *Cell Physiol Biochem* 43:1777–1789.
37. Sokabe T, Fukumi-Tominaga T, Yonemura S, Mizuno A, Tominaga M (2010) The TRPV4 channel contributes to intercellular junction formation in keratinocytes. *J Biol Chem* 285:18749–18758.
38. Lim L, Manser E, Leung T, Hall C (1996) Regulation of phosphorylation pathways by p21 GTPases. The p21 Ras-related Rho subfamily and its role in phosphorylation signalling pathways. *Eur J Biochem* 242:171–185.
39. Watanabe N, Kato T, Fujita A, Ishizaki T, Narumiya S (1999) Cooperation between mDia1 and ROCK in Rho-induced actin reorganization. *Nat Cell Biol* 1:136–143.
40. Hotulainen P, Lappalainen P (2006) Stress fibers are generated by two distinct actin assembly mechanisms in motile cells. *J Cell Biol* 173:383–394.
41. Kostic A, Sheetz MP (2006) Fibronectin rigidity response through Fyn and p130Cas recruitment to the leading edge. *Mol Biol Cell* 17:2684–2695.
42. Xu D, et al. (2007) Involvement of Fyn tyrosine kinase in actin stress fiber formation in fibroblasts. *FEBS Lett* 581:5227–5233.
43. Thompson WR, et al. (2013) Mechanically activated Fyn utilizes mTORC2 to regulate RhoA and adipogenesis in mesenchymal stem cells. *Stem Cells* 31:2528–2537.
44. Canobbio I, et al. (2015) The focal adhesion kinase Pyk2 links Ca2+ signalling to Src family kinase activation and protein tyrosine phosphorylation in thrombin-stimulated platelets. *Biochem J* 469:199–210.
45. Franco SJ, et al. (2004) Calpain-mediated proteolysis of talin regulates adhesion dynamics. *Nat Cell Biol* 6:977–983.
46. Kulkarni S, Saido TC, Suzuki K, Fox JEB (1999) Calpain mediates integrin-induced signaling at a point upstream of Rho family members. *J Biol Chem* 274:21265–21275.
47. Undyala VV, et al. (2008) The calpain small subunit regulates cell-substrate mechanical interactions during fibroblast migration. *J Cell Sci* 121:3581–3588.
48. Uhlén M, et al. (2015) Proteomics. Tissue-based map of the human proteome. *Science* 347:1260419.
49. Győrffy B, et al. (2010) An online survival analysis tool to rapidly assess the effect of 22,277 genes on breast cancer prognosis using microarray data of 1,809 patients. *Breast Cancer Res Treat* 123:725–731.
50. Friedl P, Alexander S (2011) Cancer invasion and the microenvironment: Plasticity and reciprocity. *Cell* 147:992–1009.
51. Paszek MJ, et al. (2005) Tensional homeostasis and the malignant phenotype. *Cancer Cell* 8:241–254.
52. Kim MH, et al. (2016) Actin remodeling confers BRAF inhibitor resistance to melanoma cells through YAP/TAZ activation. *EMBO J* 35:462–478.
53. Gupton SL, Waterman-Storer CM (2006) Spatiotemporal feedback between actomyosin and focal-adhesion systems optimizes rapid cell migration. *Cell* 125:1361–1374.
54. Berdeaux RL, Díaz B, Kim L, Martin GS (2004) Active Rho is localized to podosomes induced by oncogenic Src and is required for their assembly and function. *J Cell Biol* 166:317–323.
55. Berridge MJ, Lipp P, Bootman MD (2000) The versatility and universality of calcium signalling. *Nat Rev Mol Cell Biol* 1:11–21.
56. Etienne-Manneville S, Hall A (2002) Rho GTPases in cell biology. *Nature* 420:629–635.
57. Coste B, et al. (2013) Gain-of-function mutations in the mechanically activated ion channel PIEZO2 cause a subtype of distal arthrogryposis. *Proc Natl Acad Sci USA* 110: 4667–4672.
58. McMillin MJ, et al.; University of Washington Center for Mendelian Genomics (2014) Mutations in PIEZO2 cause Gordon syndrome, Marden-Walker syndrome, and distal arthrogryposis type 5. *Am J Hum Genet* 94:734–744.